Subgrid-scale backscatter after the shock-turbulence interaction

Daniel Livescu and Zhaorui Li

Citation: **1793**, 150009 (2017); doi: 10.1063/1.4971738
View online: http://dx.doi.org/10.1063/1.4971738
View Table of Contents: http://aip.scitation.org/toc/apc/1793/1
Published by the American Institute of Physics

Subgrid-scale backscatter after the shock-turbulence interaction

Daniel Livescu[1,a)] and Zhaorui Li[1]

[1]*CCS-2, Los Alamos National Laboratory, Los Alamos, NM, 87544 USA*

[a)]Corresponding author: livescu@lanl.gov

Abstract. The statistics of the subgrid scales (SGS) are studied in the context of Large Eddy Simulations (LES) of turbulence after the interaction with a nominally normal shock wave. In general, in practical applications, the shock wave width is much smaller than the turbulence scales and the upstream turbulent Mach number is modest. In this case, recent high resolution shock-resolved Direct Numerical Simulations (DNS) (Ryu and Livescu, J. Fluid Mech., 756, R1, 2014) show that the interaction can be described by the Linear Interaction Approximation (LIA). By using LIA to alleviate the need to resolve the shock wave, DNS post-shock data can be generated at much higher Reynolds numbers than previously possible. Here, such results with Taylor Reynolds number ≈ 180 are used for an analysis of the SGS backscatter properties. In particular, it is shown that the interaction with the shock wave decreases the asymmetry of the SGS dissipation Probability Density Function (PDF) as the shock Mach number increases, with a significant enhancement in size of the regions and magnitude of backscatter.

INTRODUCTION

The interaction of a shock wave with isotropic turbulence (IT) represents a basic problem for studying some of the phenomena associated with high speed flows, such as hypersonic flight, supersonic combustion and Inertial Confinement Fusion (ICF). In general, the shock width is much smaller than the turbulence scales, even at low shock Mach numbers, M_s, and it becomes comparable to the molecular mean free path at high M_s values. When there is a large scale separation between the shock wave width and turbulence, viscous effects become negligible during the interaction. If, in addition, the turbulent Mach number, M_t, of the upstream turbulence is small, nonlinear effects can also be neglected during the interaction. In this case, the interaction can be treated analytically using the linearized Euler equations and Rankine-Hugoniot jump conditions. This is known as the Linear Interaction Approximation (LIA) [1]. Recently, Ryu and Livescu [2], using high resolution fully resolved Direct Numerical Simulations (DNS) extensively covering the parameter range, have shown that the DNS results converge to the LIA solutions as the ratio δ/η, where δ is the shock width and η is the Kolmogorov microscale of the upstream turbulence, becomes small, even at low Reynolds numbers, Re, provided the M_t is small enough. The results reconcile a long time open question about the role of the LIA theory and establish LIA as a reliable prediction tool for low M_t shock-turbulence interaction problems. Furthermore, when there is a large separation in scale between the shock and the turbulence, the exact shock profile is no longer important for the interaction, so that LIA can be used to predict arbitrarily high M_s interaction problems, when DNS are not feasible.

The shock-turbulence interaction has been traditionally studied in an open-ended domain, with the turbulence fed through the inlet plane encountering a stationary shock at some distance from the inlet. This approach is very expensive even when a shock capturing scheme is used and limited to low Reynolds numbers. However, the range of the achievable Re values can be significantly increased if, instead, one uses the LIA theory to generate the post-shock fields. In order to be able to generate full 3-D fields, Refs. [2, 3] have extended the classical LIA formulas, which traditionally have been used to calculate second order moments only. Using this procedure, Refs. [2, 3] have shown profound changes in the structure of post-shock turbulence, with significant implications on turbulence modeling.

While fully resolved simulations of turbulence interacting with shock waves are prohibitively expensive at practical Re values, Large Eddy Simulations (LES) approaches have to contend with contradictory requirements for the numerical algorithms to simultaneously capture both the turbulence and the shocks. Thus, turbulence simulations re-

Shock Compression of Condensed Matter - 2015
AIP Conf. Proc. 1793, 150009-1–150009-5; doi: 10.1063/1.4971738
Published by AIP Publishing. 978-0-7354-1457-0/$30.00

quire the minimization of numerical dissipation for small scale representation, while the shocks require increased local dissipation to regularize the algorithm [4]. Explicit subgrid models also need to account for the presence of the shock. Yet, available high *Re* data necessary to investigate the subgrid scales (SGS) properties and test the LES models are scarce. This study aims at using the novel procedure proposed by Ryu and Livescu [2] to generate high *Re* post-shock data and study the changes in the SGS backscatter properties following the shock interaction. The results presented are concerned with the state of the turbulent fields after the interaction with the shock wave, as they represent the initial or boundary conditions, depending on the reference frame used, for the evolution away from the shock wave.

Numerical Approach

High *Re* post-shock DNS data are generated by first performing triply periodic forced compressible isotropic turbulence (IT) simulations using the linear forcing method [5]. This forcing method has the advantage of specifying the Kolmogorov micro scale, η, and ratio of dilatational to solenoidal kinetic energies, χ, at the outset. Here, we present results from simulations with Taylor Reynolds number, $Re_\lambda \approx 180$, $\chi = 0.01$ (quasi-vortical turbulence), and $M_t = 0.05$. The fluid is a perfect gas with the ratio of specific heats, $\gamma = 1.4$, Prandtl number, $Pr = 0.7$, and viscosity varying with temperature as $\mu \sim T^{0.75}$. The simulation domain is 2π on each side and corresponds to a mesh size of 512^3. The resulting turbulent fields are passed through the generalized LIA formulas [2, 3] to obtain 3-D post-shock turbulence.

In order to examine the properties of the subgrid scales, the post-shock fields are filtered using a Gaussian filter. All results presented are obtained in a region after the streamwise Reynolds stress reaches is maximum amplification, which occurs approximately at $k_0 x = \pi$. Here, $k_0 = 1$ is the wavenumber corresponding to the peak of the turbulent kinetic energy spectrum in the triply periodic simulation. After $k_0 x = \pi$, the variations in the mean fields become small in a corresponding shock-tube DNS, so that the contributions from the mean flow to the turbulence quantities discussed here are small. Physically, this location corresponds to the end of the inviscid adjustment of the acoustic component, following the shock-turbulence interaction, after which the LIA statistics become spatially constant. The region of agreement between DNS and LIA can be extended into this constant regime, provided that δ/η and M_t are small enough, since the eddy turnover time and, consequently, the decay distance increase with decreasing M_t at fixed Re_λ [2]. Note that features of the evolution away from the shock, like return to isotropy, cannot be captured by the LIA solutions. However, such effects due to nonlinear interactions can be made arbitrarily small by decreasing M_t.

Results

The usual picture of an energy cascade typically holds in a statistically-averaged sense; locally the energy can be transferred from large to small scales, corresponding to the classical energy cascade, as well as from the small scales back to the large scales, i.e. "backscatter". In simple homogeneous flows, the up-scale and down-scale energy fluxes can be explicitly calculated for each wavenumber (e.g. [6]). In the inertial range, such energy transfers are expected to be mostly local under stationary or weakly non-stationary conditions [7], with most of the transfer occurring in the forward (large to small scales) direction. The dominance of the "forwardscatter" should increase as the scale approaches the viscous range. However, after rapid changes, for example due to geometry, reactions, etc. the backscatter process can substantially increase [8]. In LES approaches, the SGS backscatter acts as a source term in the kinetic energy equation and poses significant difficulties in maintaining stable computations. Many of the simple SGS models do not account for backscatter and properly describing this phenomenon is an active area of research [8].

In a typical LES approach, the transport equation for the filtered or resolved kinetic energy, $\widetilde{k} = (\widetilde{u}_j\,\widetilde{u}_j)/2$, is:

$$\frac{\partial}{\partial t}(\bar{\rho}\,\widetilde{k}) + (\bar{\rho}\,\widetilde{k}\,\widetilde{u}_j)_{,j} = \left(\widetilde{u}_i\,\bar{\sigma}_{ij} - \widetilde{u}_i\,\tau_{ij} - \bar{p}\,\widetilde{u}_j\right)_{,j} + \bar{p}\,\widetilde{S}_{kk} - \bar{\sigma}_{ij}\widetilde{S}_{ij} - \bar{\rho}\,\epsilon_{SGS} \tag{1}$$

The filtering is defined as $\bar{f}(\boldsymbol{x}) = \int_{-\infty}^{\infty} f(\boldsymbol{x}')G(\boldsymbol{x},\boldsymbol{x}';\Delta_f)d\boldsymbol{x}'$, where $\boldsymbol{x}$ represents the position, G is the kernel of the LES filter and Δ_f is the characteristic filter size. An analogous Favre filtering is defined as $\widetilde{f} = \overline{\rho f}/\bar{\rho}$. For simplicity, the filter used here is a simple three-dimensional Gaussian filter. The other terms in equation (1) represent the filtered viscous stress tensor, $\bar{\sigma}_{ij}$, the strain rate of the Favre-filtered velocity, $\widetilde{S}_{ij} = \frac{1}{2}(\widetilde{u}_{i,j} + \widetilde{u}_{j,i})$, residual stress tensor, $\bar{\tau}_{ij} = \bar{\rho}(\widetilde{u_i u_j} - \widetilde{u}_i\,\widetilde{u}_j)$, and SGS dissipation

$$\epsilon_{SGS} = -\bar{\tau}_{ij}\widetilde{S}_{ij}/\bar{\rho} \tag{2}$$

The SGS dissipation appears with opposite sign in the transport equation for the subgrid kinetic energy, $k_{SGS} = \bar{\tau}_{jj}/(2\bar{\rho}) = (\widetilde{u_j u_j} - \widetilde{u}_j \widetilde{u}_j)$:

$$\frac{\partial}{\partial t}(\bar{\rho}\, k_{SGS}) + (\bar{\rho}\, k_{SGS}\, \widetilde{u}_j)_{,j} = \left[-\bar{\Phi}_{jkk}/2 - (\overline{u_i \sigma_{ij}} - \widetilde{u}_i\, \bar{\sigma}_{ij}) - (\overline{p u_j} - \bar{p}\, \widetilde{u}_j)\right]_{,j} + 2(\overline{p S_{kk}} - \bar{p}\, \widetilde{S}_{kk}) - (\overline{\sigma_{ij} S_{ij}} - \bar{\sigma}_{ij} \widetilde{S}_{kk}) + \bar{\rho}\, \epsilon_{SGS} \tag{3}$$

where $\bar{\Phi}_{ijk} = \bar{\rho}\, \widetilde{u_i u_j u_k} - \bar{\rho}\, \widetilde{u}_i\, \widetilde{u}_j\, \widetilde{u}_k - \widetilde{u}_i\, \bar{\tau}_{jk} - \widetilde{u}_j\, \bar{\tau}_{ik} - \widetilde{u}_k\, \bar{\tau}_{ij}$.

The interaction with the shock wave preferentially amplifies the transverse components of the rotation and strain rate tensors together with an M_s dependent symmetrization of the Probability Density Function (PDF) of the longitudinal derivative of the velocity components, consistent with a tendency towards a local axisymmetric state [2, 3]. Thus, the strain rate tensor contribution to the subgrid dissipation is expected to become more symmetrical as M_s increases, resulting in a significant increase in regions with negative ϵ_{SGS} or backscatter. Indeed, Figure 1 compares the distribution of backscatter between IT ($M_s = 0$) and after the interaction with a $M_s = 4$ shock wave. In IT, fowardscatter dominates, but backscatter increases significantly after the interaction with the shock wave.

The filter size used for this figure ($\Delta_f = 1.1547$) is close to the viscous scales. As the filter size approaches the viscous range, the forwardscatter is expected to become more and more important in fully developed IT, together with the increase in viscous dissipation. Conversely, if the filter size is in the inertial range, the fowardscatter, while still dominant, should decrease its relative importance. After the interaction with the shock wave, this would translate in a greater increase in backscatter at large filter sizes (figure 2). Nevertheless, the significant backscatter activity corresponding to $\Delta_f = 1.1547$ indicates changes at all scales after the interaction with the shock wave. The rest of the figures use a filter size $\Delta_f = 4$.

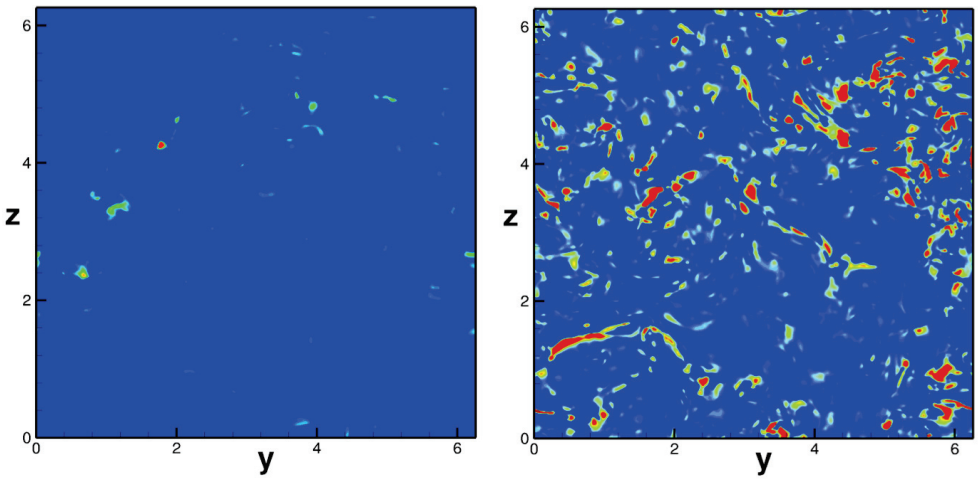

FIGURE 1. Distribution and magnitude of backscatter (negative values of SGS dissipation) in a) IT and b) in the transverse plane corresponding to the maximum amplification of the streamwise Reynolds stress ($k_0 x = \pi$) after the interaction with a $M_s = 4$ shock wave. Blue regions correspond to positive ϵ_{SGS}, while green to yellow to red denote regions with increasing magnitude of negative ϵ_{SGS}.

Figure 3a) compares the PDF of the SGS dissipation between IT and post-shock data at several M_s values. As explained above, in IT, the regions with backscatter and the magnitude of the negative SGS dissipation are limited and the PDF is strongly skewed towards positive values. However, post-shock turbulence exhibits a more symmetrical PDF and a strong increase in the variance at higher M_s values. This indicates that both the number of points with backscatter and the magnitude of backscatter increase, in an M_s dependent manner, after the interaction with the shock. The number of points with backscatter increases fast at small M_s values and seems to reach a plateau slightly below 40% of the total number of points at M_s approximately 4.

In previous studies of compressible and reacting turbulence (e.g. [8]), it was found that backscatter occurs predominantly in expansion regions and this is consistent with the IT results. This can be inferred from Figure 4a), which shows the joint PDF between ϵ_{SGS} and divergence of resolved velocity, Δ. Negative ϵ_{SGS} values occur mostly where $\Delta > 0$. However, forwardscatter can occur throughout the flow ($\epsilon_{SGS} > 0$ can be seen in both $\Delta > 0$ and $\Delta < 0$

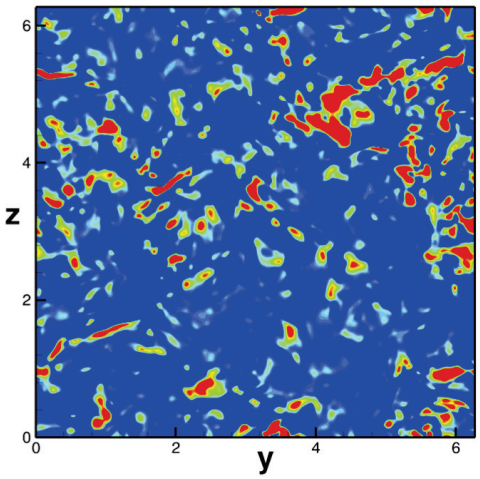

FIGURE 2. Distribution and magnitude of backscatter after the interaction with a $M_s = 4$ shock wave for a filter size $\Delta_f = 4.0$. The coloring is similar to Figure 1.

regions). After the interaction with the shock, there is a cleaner separation, with forward scatter occurring mostly in the compression regions ($\Delta < 0$), as shown in Figure 4b). Ref. [3] found that the flexion product, $\boldsymbol{u} \cdot \nabla \times \boldsymbol{\omega}$ is also largest in the compression regions immediately after the shock wave suggesting that these regions will be further amplified away from the shock, increasing the small scale activity and thus the sub-grid energy. It is then expected that backscatter should persist longer than in a usual turbulence decay. These are important changes in the structure of turbulence, which pose significant challenges for subgrid modeling of the flow.

Conclusions

Accurate simulations or measurements of turbulence interacting with shock waves are extremely challenging at high M_s and Re values, so that data necessary for testing and calibrating turbulence models are scarce. Recent high resolution DNS extensively covering the parameter space [2] show that, when there is a large scale separation between the turbulence and the shock wave width and the upstream turbulence intensity is small, the interaction between a shock wave and isotropic turbulence (IT) can be described by the Linear Interaction Approximation (LIA). Such interaction conditions occur in many practical applications. While Refs. [2, 3] open the possibility of using shock-captured turbulence-resolved simulations as an accurate tool for shock-turbulence interaction problems when the scale separation is large enough, the M_s and Re values attainable are still limited in such simulations available in the literature.

Following Ref. [3], the generalized LIA relations are used to generate high M_s and Re post-shock turbulence data at values inaccessible to both shock-capturing / turbulence resolving simulations and experimental realizations. Here, the post-shock turbulence fields are filtered to examine the backscatter properties of the subgrid scales, relevant to LES-type turbulence modeling. The interaction with the shock wave leads to an M_s dependent symmetrization of the PDF of the longitudinal derivative of the velocity components, corresponding to a tendency towards an axisymmetric local state [2]. In turn, this corresponds to an M_s dependent symmetrization of the SGS dissipation PDF as well as a large increase in the variance of ϵ_{SGS}. Thus, the interaction with the shock wave results in a significant enhancement in size of the regions and magnitude of backscatter. As the shock Mach number increases, the number of points with backscatter seems to plateau at slightly below 40% of the total number of points at M_s approximately 4. These points occur mostly in the expansion regions, while forward scatter corresponds mostly to compression regions after the interaction with the shock wave. These are profound changes in the structure of turbulence due to the interaction with the shock wave, which pose important challenges for subgrid modeling of this flow.

ACKNOWLEDGMENTS

Los Alamos National Laboratory is operated by Los Alamos National Security, LLC for the US Department of Energy NNSA under Contract No. DE-AC52-06NA25396. Computational resources were provided by the LANL Institutional

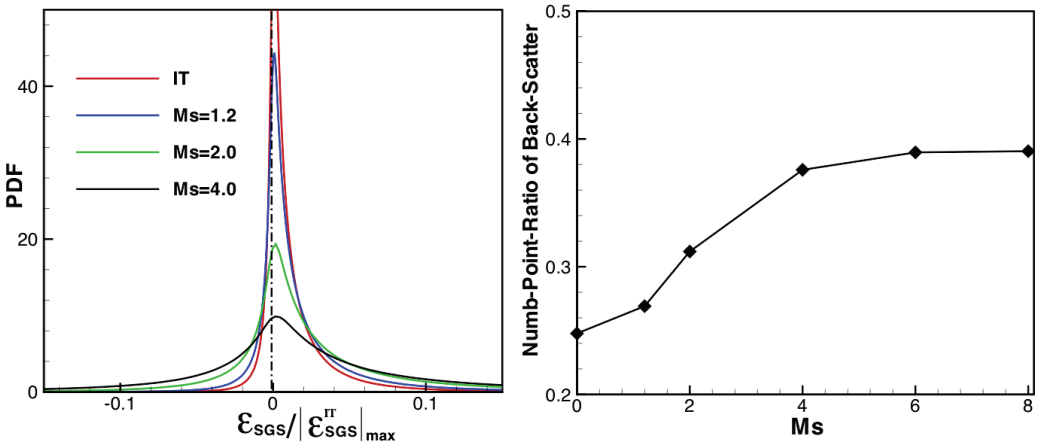

FIGURE 3. a) PDF of ϵ_{SGS} normalized by the maximum IT values for IT and after the interaction with the shock wave for several M_s values and b) The percentage of points with negative ϵ_{SGS} values as a function of M_s. Here $M_s = 0$ corresponds to IT, and the smallest shock Mach number value considered for post-shock turbulence is $M_s = 1.2$.

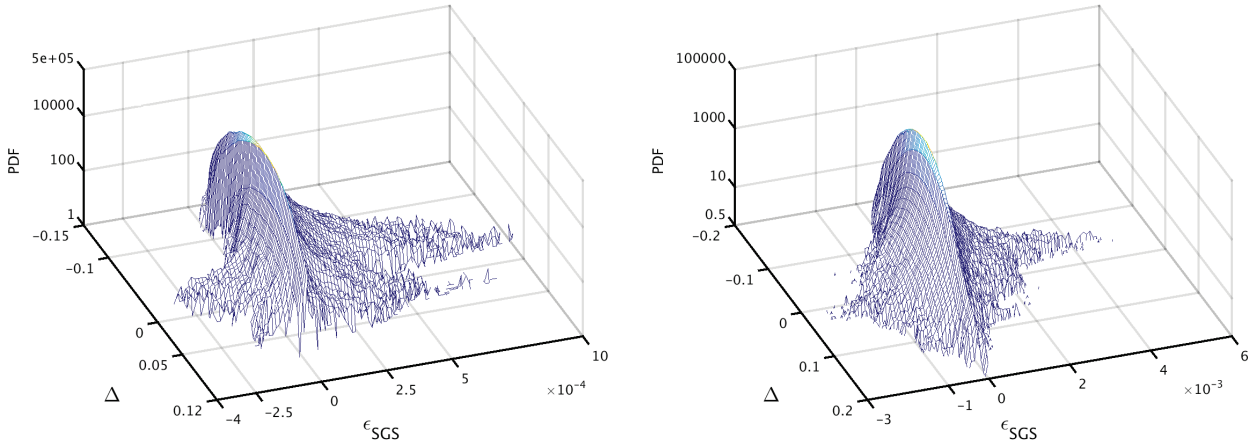

FIGURE 4. Joint PDF of ϵ_{SGS} and divergence of velocity, Δ in a) IT and b) after the interaction with a $M_s = 4$ shock wave.

Computing (IC) Program and Sequoia Capability Computing Campaign at Lawrence Livermore National Laboratory.

REFERENCES

[1] K. Mahesh, S. Lele, and P. Moin, J. Fluid Mech. **334**, 353–379 (1997).
[2] J. Ryu and D. Livescu, J. Fluid Mech. **756**, p. R1 (2014).
[3] D. Livescu and J. Ryu, Shock Waves http://dx.doi.org/10.1007/s00193–015–0580–5 (2015).
[4] E. Johnsen, J. Larrson, A. Bhagatwala, W. Cabot, P. Moin, B. Olson, P. Rawat, S. Shankar, B. Sjogreen, H. Yee, X. Zhong, and S. Lele, J. Comp. Phys. **229**, 1213–1237 (2010).
[5] M. Petersen and D. Livescu, Phys. Fluids **22**, p. 116101 (2010).
[6] J. Brasseur and C. Wei, Phys. Fluids **6**, 842–870 (1994).
[7] G. Eyink, Physica D **207**, 91–116 (2005).
[8] J. O'Brien, J. Urzay, M. Ihme, P. Moin, and A. Saghafian, J. Fluid Mech **743**, 554–584 (2014).